Final Technical Report: Shock Induced Chemistry: Application and Development of Ultrafast Nonlinear Probes of the Dynamics of Molecules in Solids and Flames (N00014-89-J-1119)

Michael D. Fayer
Department of Chemistry
Stanford University, Stanford, CA 94305

Under the grant N00014-89-J-1119 we have made significant progress in a number of areas that have led to increased understanding of dynamics in solids and flames and in the development of new experimental techniques and associated theory for the investigation of condensed matter and gas phase systems. This work will be briefly summarized in this section. A list of publications that have resulted from the research supported by this grant follows.

A. Surface Selective Transient Grating Experiments: Heat Flow at Interfaces

The laser induced transient grating technique which has been expanded in areas of application and sophistication over the last decade has been successfully applied to the investigation of a wide variety of transient processes in liquids, solids, and gases. Previous theoretical treatments of transient gratings [1] were developed by direct analogy with the diffraction from transparent volume holograms [2,3] where the general method of slowly varying amplitudes was utilized. The grating was assumed to be constant in amplitude throughout the sample and the probe beam was assumed to be weakly absorbed. Recent experimental investigations on samples with very high optical densities [4], e.g. metals or absorbing dielectrics with spatially nonuniform gratings, demonstrated that further theoretical development is required in which

the effects of surfaces are included. Recent work in our laboratory has provided such a formalism for describing both reflection and transmission geometries of diffraction where surface effects are specifically considered for samples with or without a high optical density and an arbitrary grating excitation profile. [5] The essential features of the transient grating diffraction efficiency are given by

$$\eta^{R}(t) \quad \alpha \quad \left| \int_0^{\ell} e^{2ik_o x} \quad \Delta\epsilon(x,t) \; dx \right|^2, \tag{1}$$

for the reflected geometry and

$$\eta^{T}(t) \quad \alpha \quad \left| \int_0^{\ell} \Delta\epsilon(x,t) \; dx \right|^2, \tag{2}$$

for the transmitted geometry. The probe wave-vector in vacuum is written k_o and the grating amplitude or peak to null change in the dielectric constant is denoted $\Delta\epsilon$. The reflected diffracted geometry (Eq. 1) has an exponential term that localizes the sampling region near the incident interface while the transmitted geometry is simply the average of the grating amplitude throughout the bulk.

By analyzing different diffraction geometries, the transient grating method can provide information on the spatial distribution of material excitations. This is illustrated with experimental results from a thin film (220nm) of the high temperature superconductor $YBa_2Cu_3O_{7-x}$ (YBCO) on a MgO(100) substrate. Absorption of the 561 nm laser grating excitation beams by the superconductor produces electronic excitations that rapidly damp (~1ps) by the generation of a large number of phonons. This incoherent jump in the phonon population is heat, and the result is a sinusoidal heat pattern. The sinusoidal heating generates a sinusoidal density variation, and since the index of

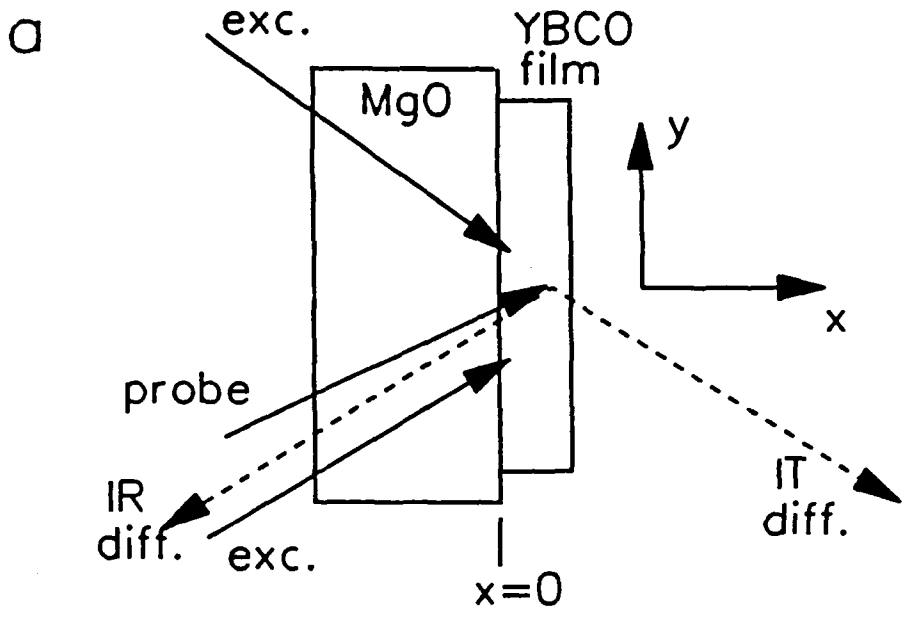

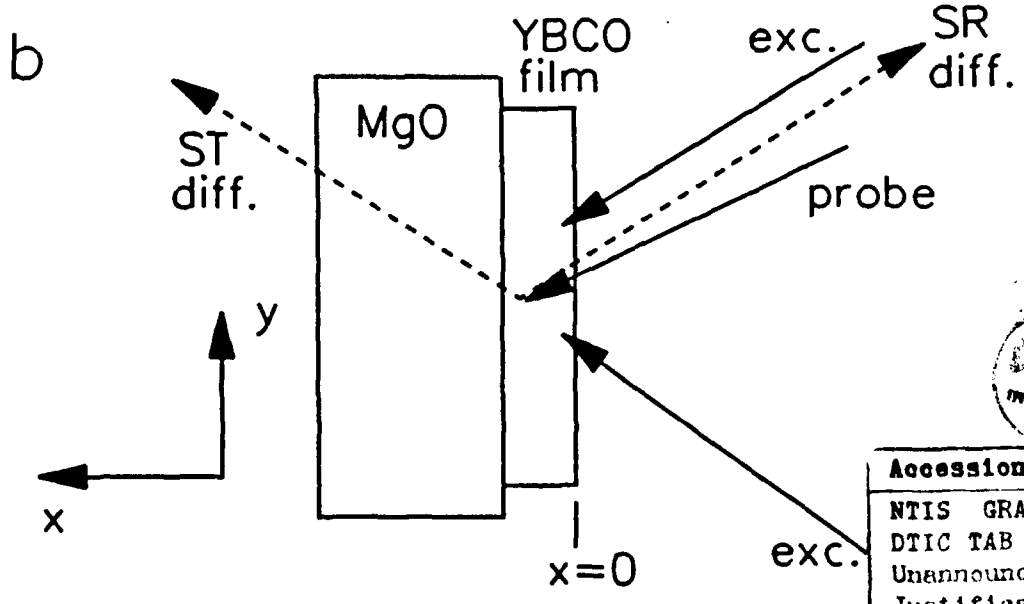

Figure 1

refraction is density dependent (opto-elastic constant), a holographic grating is produced.

The heat undergoes diffusion and the impulsive heat deposition drives multiple acoustic waveguide modes [6]. The probe beam is temporally delayed and diffracted from the transient holographic grating. Four different transient grating geometries are shown in Fig. 1. When one looks at the reflected geometries (denoted refl. in Fig. 1), the probe will selectively sample a region near the incident probe interface. In contrast, the transmission geometries (denoted trans. in Fig. 1) will sample the entire sample uniformly. The transient grating method can therefore directly and simultaneously provide information on transient processes at a surface or interface and inside the bulk of a material.

Figure 2 shows the results of the transient grating experiments at 300 K. The solid lines thru the data are theoretical fits where three dimensional diffusion is assumed. The MgO is an infinite heat sink since the thermal conductivity of MgO is several orders of magnitude higher than YBCO. To properly fit the data, a barrier limited heat flow model must be used at the MgO-YBCO interface. Several different models were considered. One was a barrier region of finite thickness inside the YBCO while another was that the temperature at the interface was a constant. Neither of these models could simultaneously fit all four data sets without individually adjusting the thermal constants between geometries. Using a surface conductivity model where the temperature gradient at the interface is proportional to the temperature difference across the interface, it was possible to simultaneously fit all four geometries. These fits are the ones given in Fig. 2.

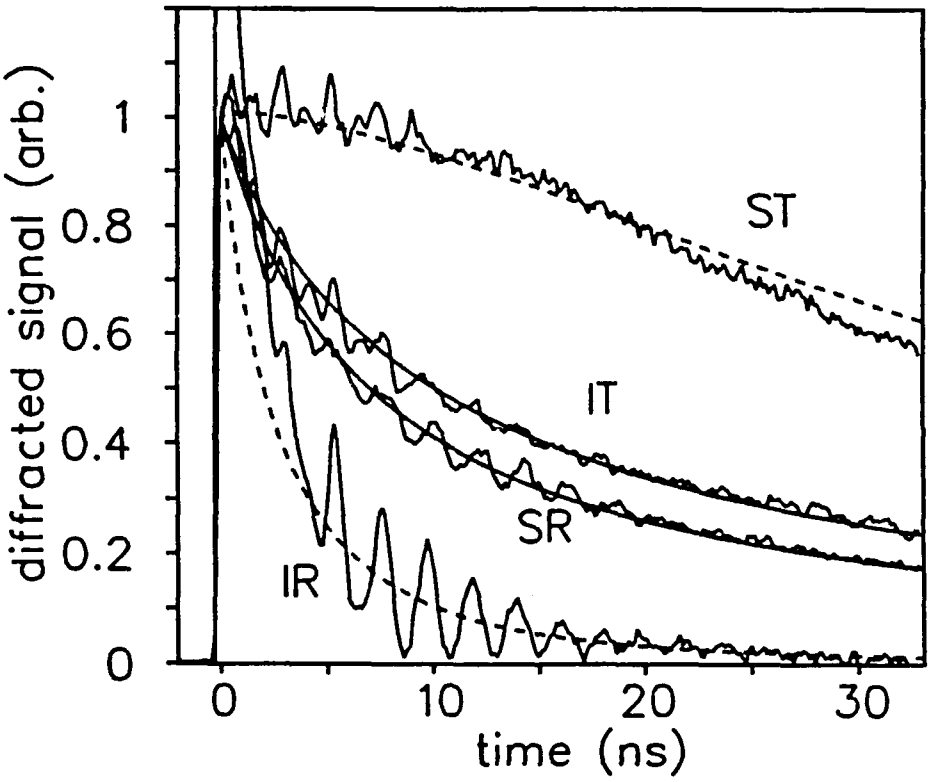
diffracted signal (arb.)
1
0.8
0.6
0.4
0.2
0
0
10
20
30
time (ns)
ST
IT
SR
IR

Figure 2

It is important to note that it was necessary to use multiple geometries to properly model the dynamics inside the material, at the surface, and at the interface. In general, thin films or boundary layers can have different properties than those of the bulk material. Since a variety of important physical phenomena occur at surfaces and interfaces and many new devices are based on thin film technology, it is important to have a technique that can nondestructively measure the properties of thin films. Conventional techniques for measuring thermal propagation in materials rely on sensors that must make intimate contact with the sample without disturbing the thermal flow itself [7,8]. This requires either large specially shaped samples or very small sensors. In either case the sample size is limited to dimensions much larger than 100 nm. Since the transient grating method described here is a remote sensing technique, the measurement process does not require physical contact with the sample. Thus the sample size need not be constrained to dimensions larger than those of the detectors and very thin materials can be studied down to atomic dimensions. This illustrates a powerful new way to study thin film, interface, and surface properties where bulk and surface effects can be measured separately. While the results described here investigate the important problem of interfacial heat flow, a wide variety of other phenomena, e. g., dynamics of molecules or concentrations of chemical species, can be studied.

B. Non-linear Optical Studies of Flames and Gas Phase Dynamics

1. Picosecond Four-Wave Mixing Experiments in Sodium-Seeded Flames

The ability to non-invasively probe the local properties of flames (e.g.,transport properties, species concentrations, temperature, reaction rates, and collision cross-sections) over small (sub-millimeter) distance scales is essential to the understanding of combustion. The advent of lasers has allowed some of these processes to be studied, and techniques such as Laser-Induced Fluorescence (LIF), Raman spectroscopy, and absorption measurements have become the mainstays of combustion research [9]. These experiments tend to be difficult to perform however, due to a combination of weak signals and a large amount of background noise (both from the flames and the laser beams themselves). For these reasons, four-wave mixing (FWM) techniques have proven quite useful in combustion research; these techniques generally provide relatively strong signals that are spatially separated from the laser beams. Coherent Anti-Stokes Raman Spectroscopy (CARS) [10] and other FWM techniques [11] have proven useful in obtaining information on steady-state flame properties such as concentration profiles. Four-, six-, and eight-wave mixing have also been used to study collision-enhanced spectra in sodium-seeded flames [12]. To study the fast time-scale dynamics of flames (such as collisions, velocity distributions, and reactions), it is necessary to perform experiments with subnanosecond laser pulses.

The picosecond transient grating [13] is a unique and powerful tool for probing fast time-scale dynamics. Previous work in this laboratory has demonstrated that the transient grating is an effective method for probing velocity distributions in low-pressure gases [14].

We have successfully applied the transient grating to the study of various Na-seeded pre-mixed flames [15].

Figure 3a shows an intensity grating (a grating in which both excitation beams are of the same polarization) decay in a Na-seeded, methane/air flame. The decay is exponential with a decay constant of 800 psec, which is much shorter than the 16 nsec Na excited-state lifetime [16]. This decay is insensitive to the grating fringe spacing, and therefore corresponds to the Na excited-state quenching rate. Figure 3b shows a polarization grating (a grating in which the excitation beams are of orthogonal linear polarizations) decay taken under the same conditions in the same flame. The differences between the two decays is striking. Whereas the intensity grating decay is smooth, the polarization grating decay shows large oscillations at the Na ground-state hyperfine-splitting frequency. More remarkably, the decay time of the polarization grating is seven times longer than that of the intensity grating at this fringe spacing. Moreover, the polarization grating decay constant is sensitive to fringe spacing. Figure 4 is a plot of this constant vs. $(2\pi/d)^2$, where d is the grating fringe spacing. The points in this plot fall along a straight line whose slope is related to the Na diffusion constant. Using these techniques, we have been able to measure four picosecond dynamic processes in various Na-seeded flames: excited-state quenching, excited-state population scattering, ground-state magnetic-sublevel population scattering, and the diffusion of Na atoms. We will soon be using these techniques to probe the dynamics of intrinsic flame species.

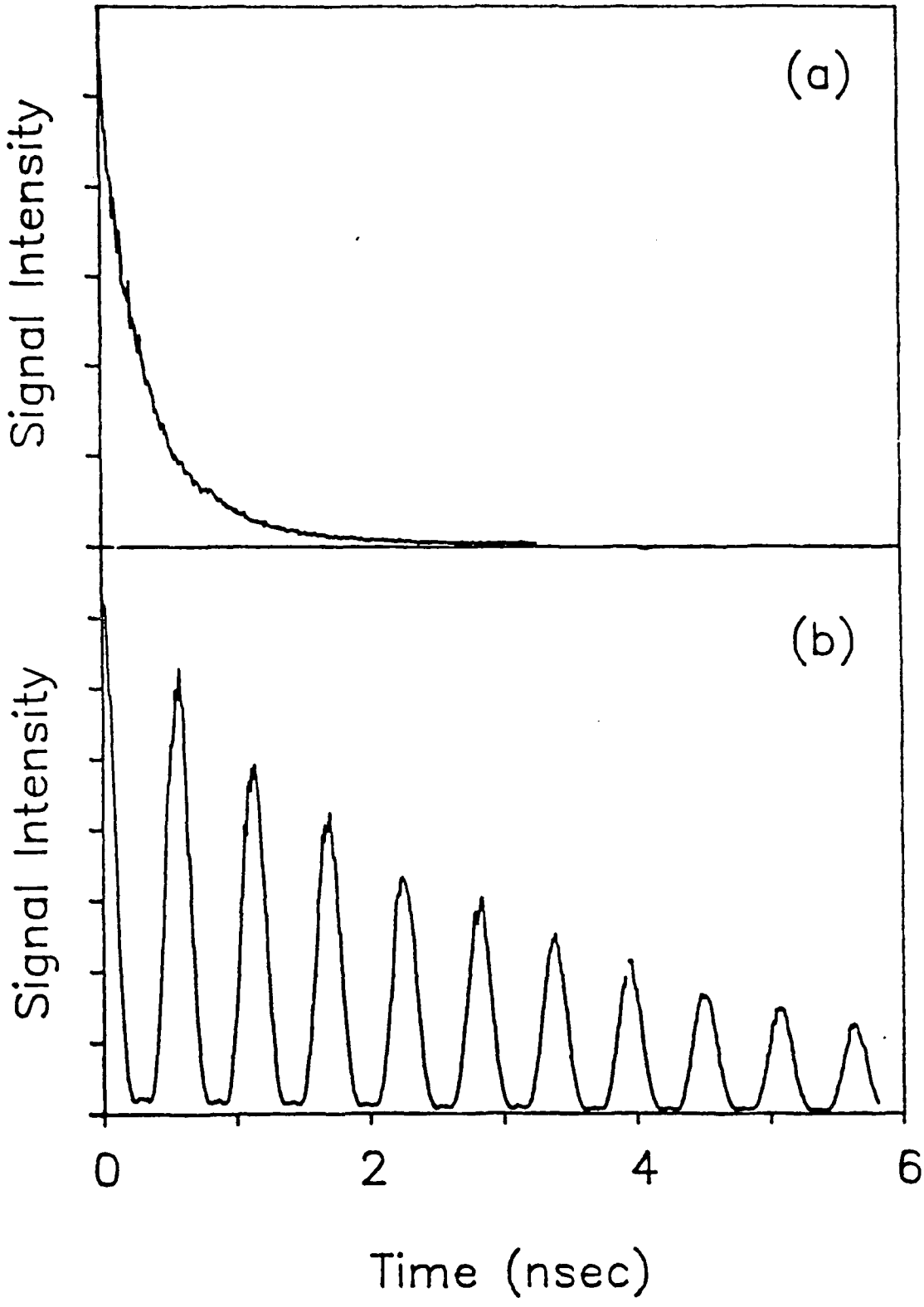

Figure 3

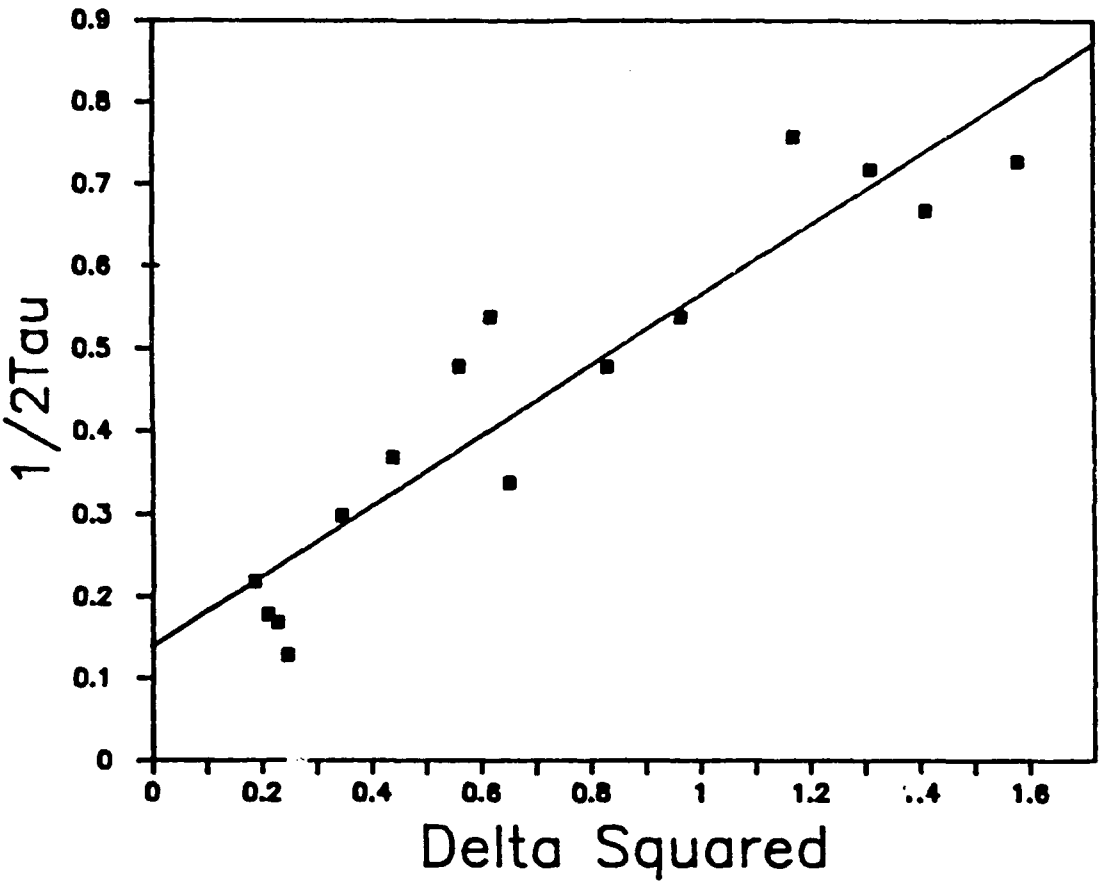
0.9
0.8
0.7
0.6
0.5
0.4
0.3
0.2
0.1
0
1/2Tau
0
0.2
0.4
0.6
0.8
1
1.2
1.4
1.6
Delta Squared

Figure 4

2. The Grating Decomposition Method

Four-wave mixing (FWM) techniques have become increasingly powerful tools for probing phenomena in all phases of matter. An important special case of FWM, the transient grating [17] (TG), has proven useful in studying a multitude of interesting processes. Although the transient grating is a versatile technique, TG data are not always simple to interpret, especially those arising from orientational gratings (gratings in which the direction of the electric field changes along each fringe; an example of this is the linear polarization grating [18], in which the excitation beams are cross-polarized). Historically, two approaches have been taken in the interpretation of orientational TG data. The first approach makes predictions based on the spatial dependence of the amplitude and direction of the grating electric field [19,20]. While this approach has the advantage of being simple and intuitive, it provides little calculational power. Even worse, electric field pictures may at times lead to unphysical predictions, such as higher-order diffraction at low excitation beam intensities.

The other approach that has been used to understand TG experiments and FWM in general [21-23] is the density matrix formalism, usually in the form of diagrammatic perturbation theory. In this formalism, Feynman diagrams are used to depict integrals that describe the couplings of material states by laser fields and the evolution of these material states in between field interventions. A weakness of this theory as it is usually applied to orientational TG experiments, however, is that spatial information about the excitation processes is not available in a form that provides physical insight. This information can be essential to the understanding and calculation of

orientational gratings and their decays for several reasons. First, decay constants must be added in a completely *ad hoc* manner; in some systems (such as gas-phase sodium atoms), the decay constants for both linear intensity gratings and linear polarization gratings are calculationally identical, even though the experimentally observed decay constants may differ greatly. Such differences arise because of the different spatial dependences of the excitation processes in each experiment. Second, this theory cannot treat secondary effects such as thermal gratings [24] or molecular alignment (such as through the nuclear Optical Kerr Effect [20]), even though these effects may be major contributors to grating signals. It is difficult to extend diagrammatic perturbation theory to treat such processes without understanding the spatial nature of the excitation process.

We have shown that it is possible, through the decomposition of excitation beam polarizations into various component polarizations, to transform diagrammatic perturbation calculations of orientational gratings into sums of linear (±45°) and circular (right and left) intensity grating calculations [25] (see Fig. 5). In each of these component intensity gratings, the two excitation beams have the same polarization, and therefore spatial information is restored. Thus spatial information (and therefore insight) is included in orientational grating calculations. We have also introduced effective two-interaction matrix elements (ETIMEs), which simplify some of the summations that must be performed in diagrammatic perturbation calculations. We have used the GDM and ETIMES to simplify the treatment of picosecond absorption and emission orientational gratings and nuclear Optical Kerr Effect orientational gratings in isotropic molecular liquids. The GDM

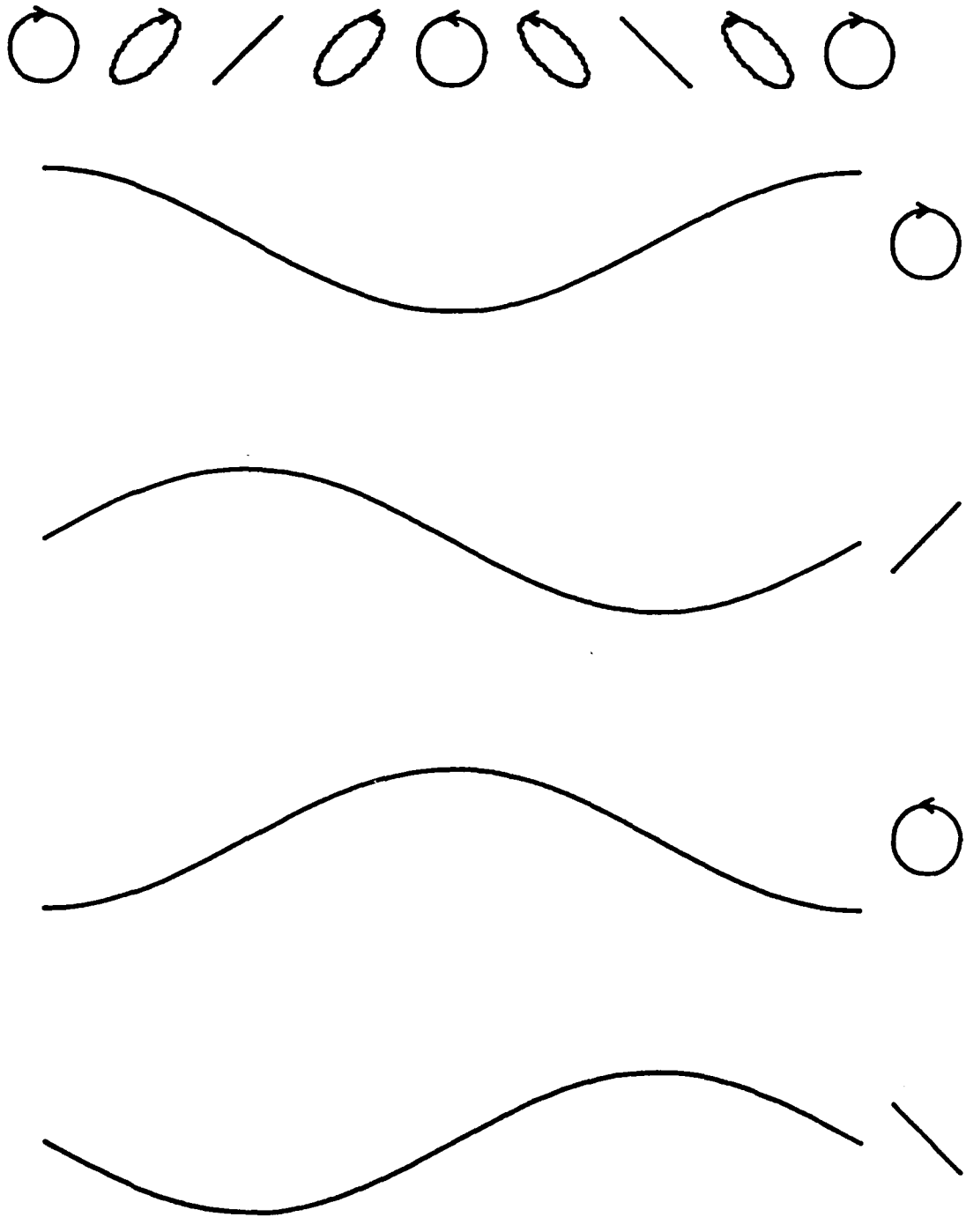

Figure 5

approach to the latter problem clears up inconsistencies that arose in previous treatments. In addition, we have successfully used the GDM and ETIMEs to treat a problem that cannot be properly treated within the confines of standard diagrammatic perturbation theory: orientational gratings of gas-phase Na atoms. We have been able to accurately model the behavior of polarization gratings on the Na D lines in low-pressure gas cells and in Na-seeded flames [26], while at the same time greatly reducing the necessary calculations. The GDM and ETIMEs will find many applications in orientational grating problems.

3. Picosecond Time-Scale Phase-Related Optical Pulses

The development of optical coherence techniques for probing the properties of systems of atoms and molecules has in many instances closely followed the path taken by nuclear magnetic resonance (NMR) techniques. In general, however, optical pulse sequences that parallel magnetic resonance have not been able to employ one important property of the pulses in most NMR sequences: well-defined phase relationships [27,28]. Without the ability to control the relative phases of ultrafast (picosecond or femtosecond) laser pulses that are separated in time, it is impossible to utilize many potentially useful experimental techniques, such as the fluorescence-detected photon echo [29] and the dipolar echo [30].

We have developed a technique that can potentially be used to phase lock any arbitrary number of ultrafast pulses [31]. In addition, this method can serve as an add-on to existing ultrafast laser systems. We have used this technique to phase-lock a pair of picosecond time scale laser pulses in order to measure the optical coherence decay of the D_1 line of sodium vapor.

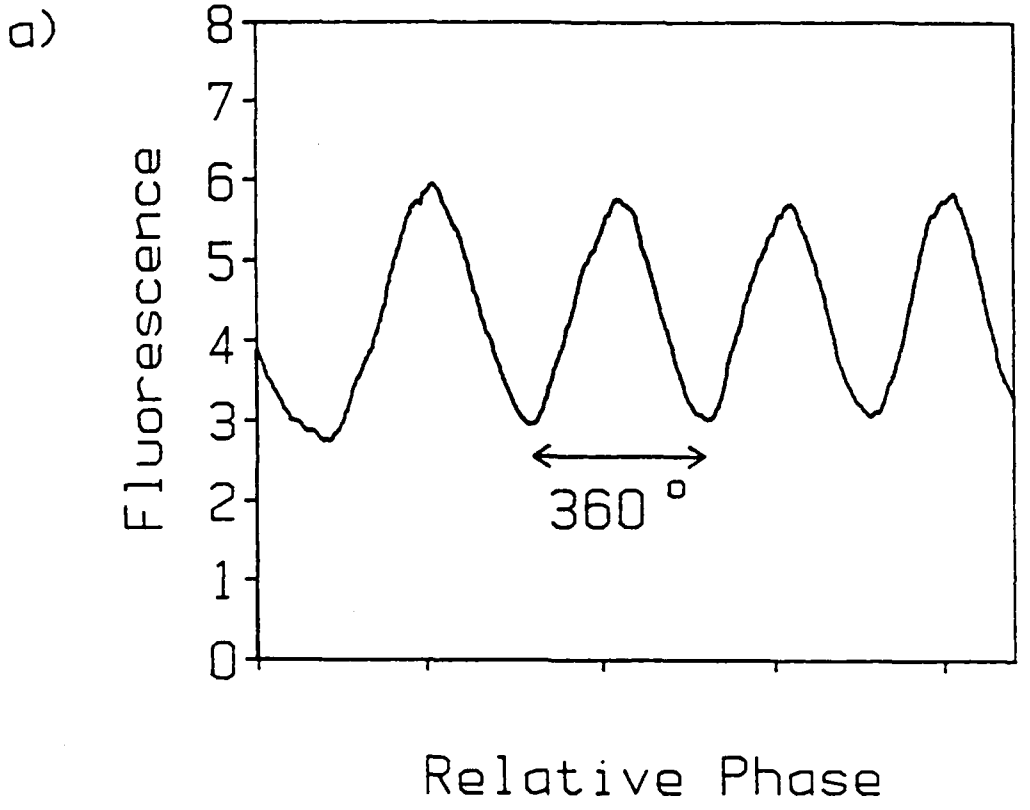
a)
Fluorescence
0
1
2
3
4
5
6
7
8
360 °
Relative Phase

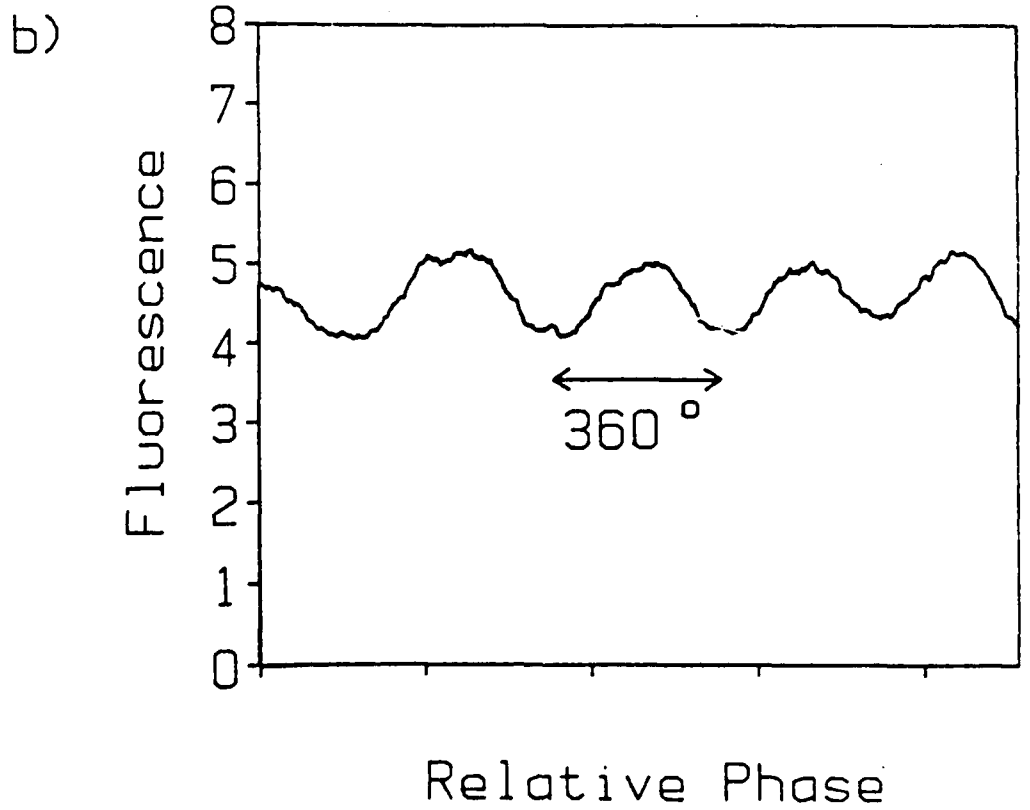
b)
Fluorescence
0
1
2
3
4
5
6
7
8
360 °
Relative Phase

Figure 6

In this experiment, a 40-psec, phase-locked, temporally separated laser pulses that are resonant with the Na D_1 transition are passed through a Na gas cell. The resultant incoherent fluorescence is monitored at a right angle to the path of the laser beams. As the relative phase between the pulses is scanned, the fluorescence from the Na cell is sinusoidally modulated. Such a scan is illustrated in Fig. 6, in which the delay time is 107 psec. By plotting the peak-null difference in the fluorescence oscillations as a function of the delay time between the pulses, we were able to plot the coherence decay of the Na. This data is illustrated in Fig. 7, along with a theoretical fit that uses no adjustable parameters. The fluorescence oscillations in Fig. 6 and the excellent fit between theory and experiment in Fig. 7 illustrate that the relative phase between the laser pulses is indeed well-defined. This method of phase-locking promises to be useful in ultrafast experiments in all phases of matter.

C. Ultrafast Dynamics in Complex Liquids

The rotational dynamics of liquids have been under intense investigation in recent years. There exists a large number of techniques for studying these dynamics, including fluorescence depolarization, dynamic light scattering , optical Kerr effect (OKE), nuclear magnetic resonance, electron spin resonance, and Raman scattering. The majority of the time domain experiments have been done on very small, simple molecules such as CS_2 [32,33]. These experiments were primarily done to investigate the ultrafast librational dynamics. The rotational diffusion of these molecules has usually been described by a single exponential.

a)

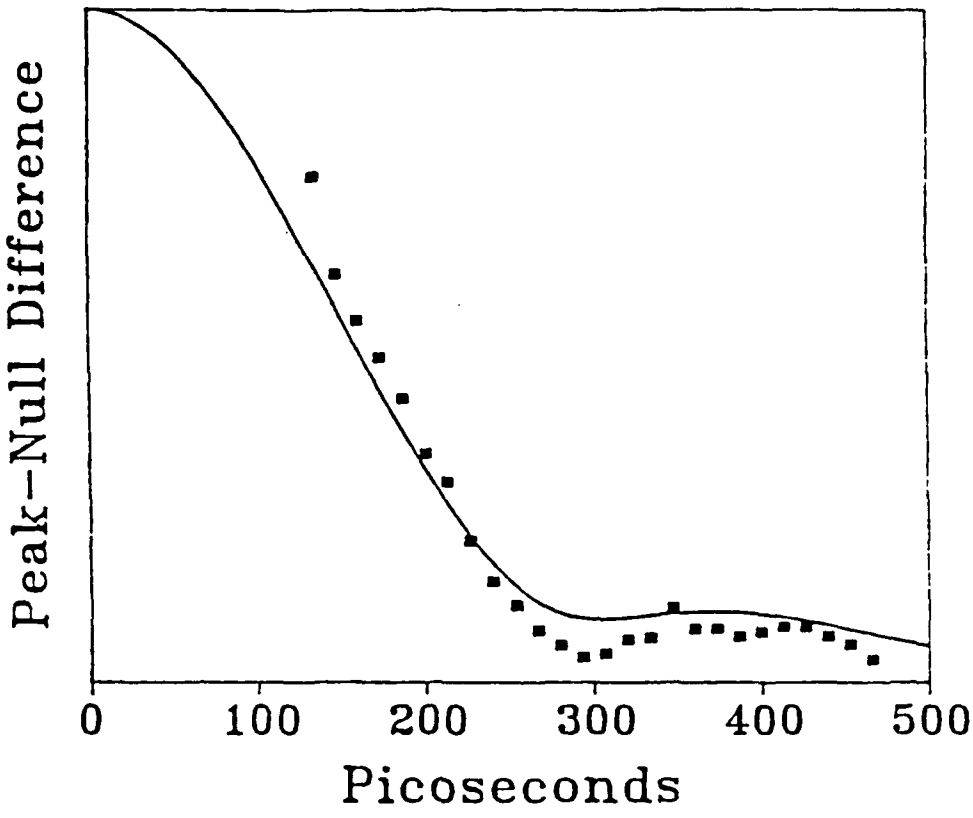
Peak-Null Difference
0
100
200
300
400
500
Picoseconds

b)

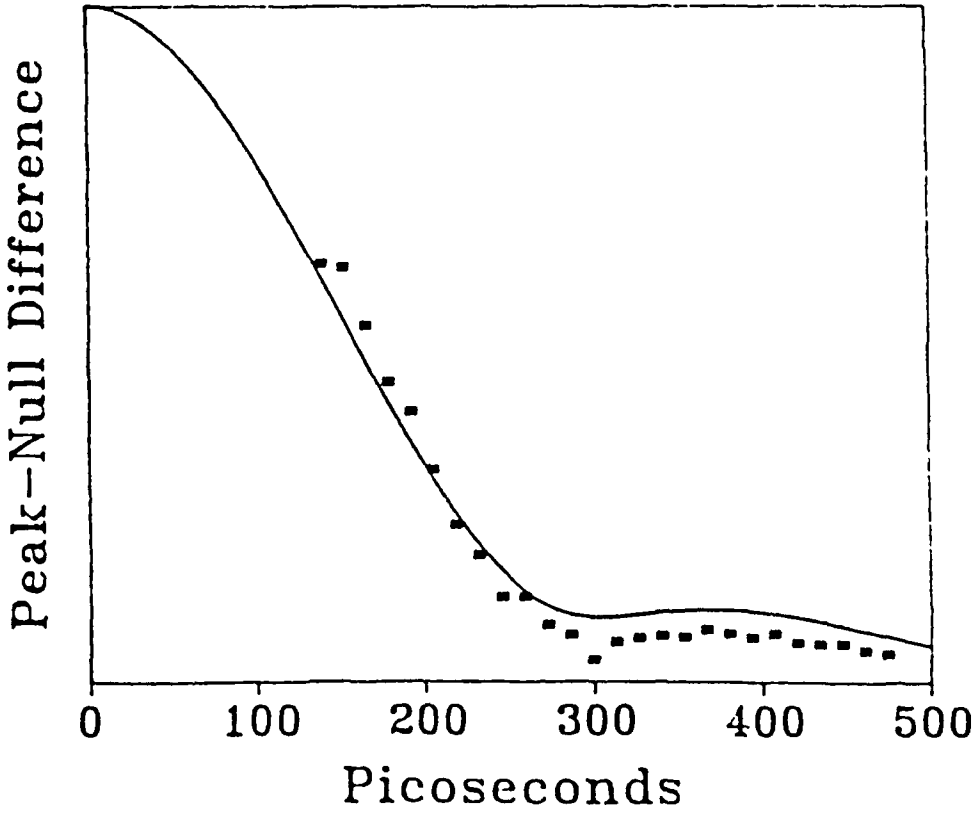
Peak-Null Difference
0
100
200
300
400
500
Picoseconds

Figure 7

The rotational dynamics of molecules has been assumed to be adequately described by a modified Debye-Stokes-Einstein (DSE) theory. This theory, which was developed to describe the dynamics of a rotating sphere in a featureless continuum, relates the rotational diffusion time τ_{rot} to the bulk viscosity of the medium, η, and the temperature, T [34].

$$\tau_{rot} \propto V_{eff}\eta/kT \qquad (3)$$

The proportionality constant, V_{eff}, is the effective volume of the molecule. Molecular reorientational motions that are described by DSE theory can be referred to as hydrodynamic.

The ultrafast component of the rotational dynamics of liquids can not be described by DSE model. At times shorter than 1-2 ps, the dynamics are dominated by librations and collision-induced (CI) phenomena. The equilibrium ensemble of librations is altered by the fsec laser pulse. The broad bandwidth of the fsec laser pulse permits coherent Raman excitation of librations of frequencies within the pulse bandwidth [35].

The experiments that are described here were performed with a subpicosecond laser system developed in our labs [36]. The output of a cw mode-locked Nd:YAG laser was pulse-compressed and frequency doubled to synchronously pump a dye laser, providing tunable 300 fs pulses at 82 MHz. A Q-switched, and mode-locked Nd:YAG laser is cavity dumped at 1.75 kHz and then frequency doubled. The 700 μJ single pulses at 532 nm are used to amplify the dye laser output. Transform-limited 150-300 fs amplified pulses of energies up to 50 μJ were obtained in the wavelength range of 560-680 nm (R6G and DCM dyes).

The OKE was studied using a transient grating technique, first

used by Eyring and Fayer [37]. The transient grating approach has a number of advantages over a pump-probe transient birefringence method, including background-free detection and the ability to separate the electronic and nuclear contributions to the OKE. As first described by Etchepare *et al* [38], and extended by Deeg and Fayer [39], physical processes having different $\chi(3)$ symmetries can be observed independently by choosing the correct polarizations for the three input beams and the signal. The nuclear contribution can be eliminated, providing observation of the electronic response (which gives the instrument response). If the electronic contribution is eliminated, direct observation of the nuclear response is permitted.

The reorientational relaxation of biphenyl showed relatively straight forward behavior [40]. At times greater than 2 ps, the reorientational dynamics of biphenyl can be described by a bi-exponential decay. The slower component corresponds to the tumbling motion of the biphenyl molecule, whereas the faster component is associated with the torsional motion of the two phenyl rings around the central C-C bond. A temperature dependence showed hydrodynamic behavior for the 66 ^{o}C temperature range studied. The ultrafast dynamics (< 2 ps) was described as a pair of overdamped oscillators, one corresponding to each of the rotational diffusion decays. Explicit linkage of the librational and rotational diffusion decays was made for the first time. Typical data are shown in Figure 8.

A similar study of the isotropic phase of the nematic liquid crystal pentylcyanobiphenyl (5CB) showed vastly more complex behavior [41-43]. There is a very slow component to the decay (up to 100 ns near the phase transition) corresponding to the motion of the microscopic

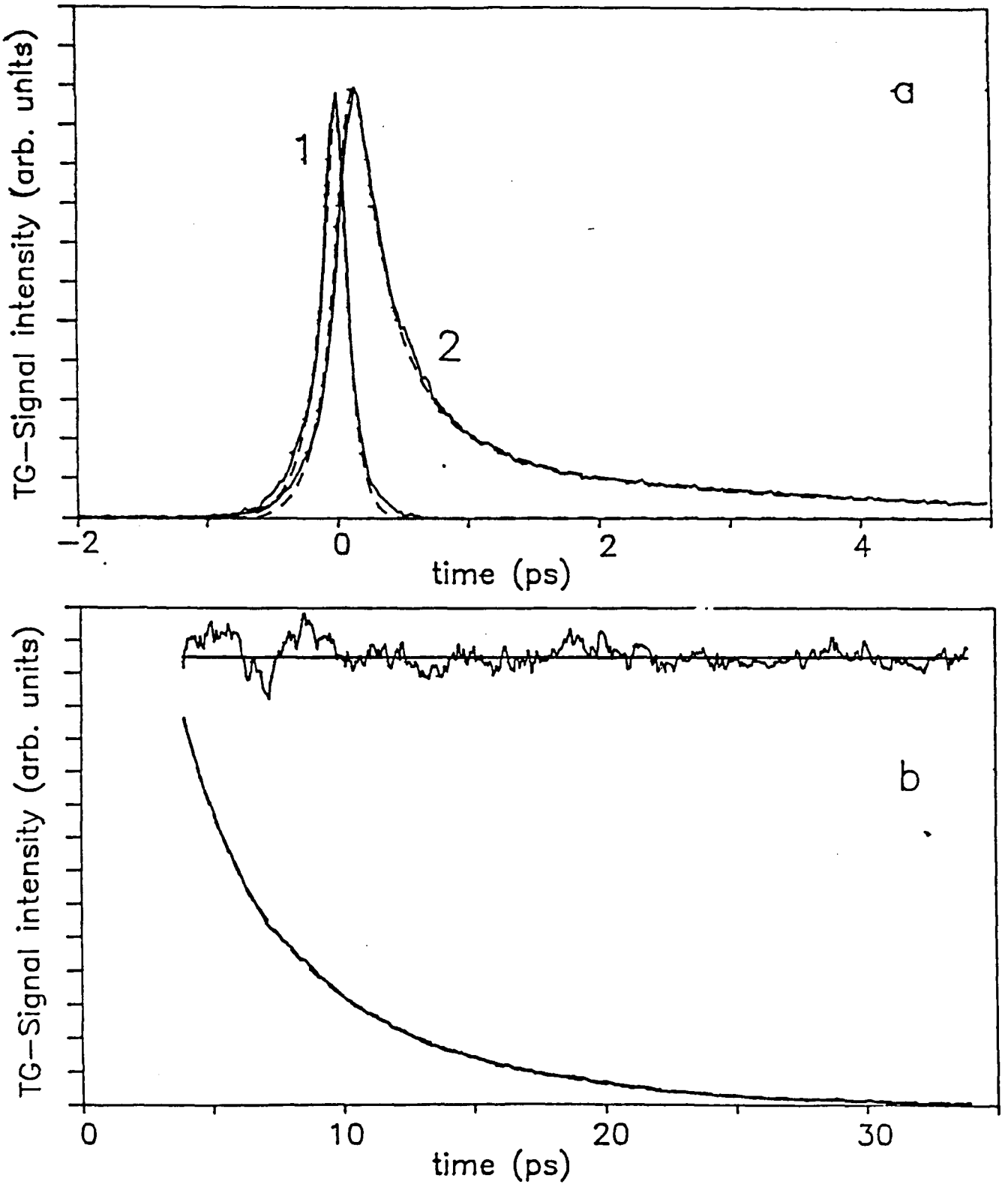
TG-Signal intensity (arb. units)
a
1
2
-2
0
2
4
time (ps)
TG-Signal intensity (arb. units)
b
0
10
20
30
time (ps)

Figure 8

psuedonematic domains. The temperature dependence of this component of the decay is well described by Landau-deGennes theory [13]

$$\tau_c \propto \eta/(T-T^*) \qquad (4)$$

where T^* is the virtual phase transition temperature. This model fits the data up to 30-35 ^oC above the phase transition. At this temperature, the size of the psuedonematic domains becomes of the order of a few molecules. In that same temperature range, all of the faster dynamics are temperature independent. This is a breakdown of DSE theory and represents a decoupling of the dynamics from the bulk viscosity. As can be seen in fig. 9, a temperature dependence in the slowest non-collective component develops at higher temperatures (i.e., when the psuedonematic domains become vanishingly small). When 5CB is put in n-heptane solutions, the collective component of the decay disappears, and the remaining components behave hydrodynamically.

A study of 2-ethyl naphthalene shows complex behavior in a simple liquid [45]. A times greater than 2 ps (after the ultrafast librational dynamics have damped out), the decay can be accurately described by a triple exponential with each component having 4 to 6 factors of e decay. Over the 80 ^oC temperature range studied, the slowest two components exhibited hydrodynamic behavior. The fastest component was temperature independent from 2-40 ^oC. In analogy to the collective motions in 5CB, this represents the domination of the fast dynamics by local structures in the liquid. These local structures have dynamics that depend on the details of the local intermolecular interactions rather than on the bulk viscosity.

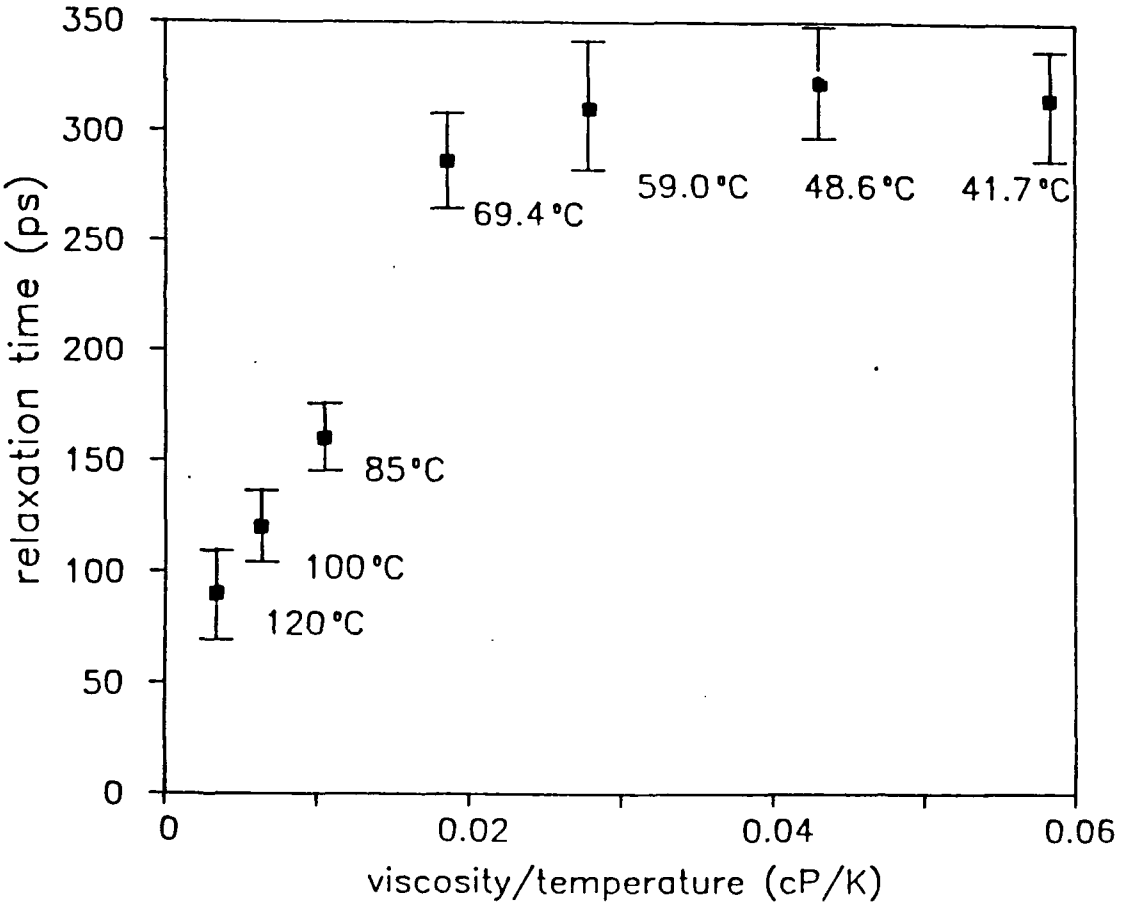
350
300
250
200
150
100
50
0
relaxation time (ps)
0
0.02
0.04
0.06
viscosity/temperature (cP/K)
120°C
100°C
85°C
69.4°C
59.0°C
48.6°C
41.7°C

Figure 9

D. Probing Disordered Solids with Variable Time Scale Optical Dephasing Measurements

Dynamics and interactions in glasses and other disordered materials such as imperfect crystals or proteins can be studied with optical line narrowing techniques applied to chromophores embedded in the disordered material. Prior to the use of optical methods, a wide variety of classical methods, such as heat capacities, were applied to the study of glasses. Results have been successfully interpreted in terms of a model of the glass potential surface described in terms of the Two Level Systems (TLS) [46,47] model. Because of the very large extent of inhomogeneous broadening in glassy systems, it is necessary to apply line narrowing methods to provide information on the dynamics and interactions of atoms and molecules with their environments.

A number of optical line narrowing methods have been developed to remove inhomogeneous broadening. Among these are hole burning, fluorescence line-narrowing, accumulated grating echoes, stimulated photon echoes, and photon echoes. The photon echo and the stimulated photon echo are the direct optical analogs of the magnetic resonance spin echo and stimulated spin echo. In magnetic resonance it is known that the spin echo measures the homogeneous dephasing time, T_2, and that the stimulated echo can have additional contributions to the dephasing time from spectral diffusion occurring on time scales slower than T_2. Until recently hole burning and fluorescence line narrowing have been the line narrowing techniques applied to the study of glasses. Various workers have defined the observables of these techniques as the homogeneous linewidth. Each technique, however, is sensitive to processes over a different range of time scales and, in general, will

yield different linewidths [48-50].

The line narrowing experiments have been treated as if they are absorption experiments using optical absorption formalisms. The line narrowed lineshape was taken to be related to the Fourier transform of the two-time transition dipole-moment correlation function. However, the two time correlation function is insufficient to describe actual line-narrowing experiments, such as hole-burning, that are performed on glasses and crystals [48]. In fact the two time correlation function description of experiments has been misleading. It indicated that all of the line narrowing experiments measured the same observable, the homogeneous line. It caused the fundamentally distinct nature of different experiments, i. e., the characteristic time scale associated with each experiment, to be absent from the theoretical treatments. Using the correct description of the different experiments makes it possible to obtain information on the broad distribution of rates of dynamical processes in complex systems [48-50].

A theoretical formalism has been developed by Berg et al. [51] and extended by Bai and Fayer [52] that relates the experimental observables in the various types of line narrowing experiments to details of the dynamics and intermolecular interactions in complex systems such as glasses. Each line-narrowing technique can be regarded as a specific case of a four-wave mixing experiment in which three input beams induce and subsequently interfere with a polarization in a medium to generate a fourth (signal) beam. The frequency domain experiments have specific time domain analogs obtained through Fourier transforms. The differences between the techniques are reduced to the timing between the pulses in the time domain description. It has also been shown that all of the

line-narrowing experiments currently being performed on glasses are describable in terms of correlation functions that are variants of the stimulated echo four time correlation function. In a stimulated echo, three pulses are applied at times, 0, τ and $\tau+T_w$. A fourth pulse, the signal, emerges at time $2\tau+T_w$. The correlation function is usually specified by the time intervals between the pulses, i.e., τ, T_w, and τ. The detailed analysis shows that the differences among the various line narrowing experiments is the duration of the interval T_w, which has a major influence on the observables in the experiments [48-52].

First consider the photon echo experiment. It is the limit of a stimulated echo experiment with $T_w=0$. The second and third pulses in the sequence are time coincident. Inhomogeneous broadening is eliminated by the echo pulse sequence. The polarization in the sample decays as the separation between the two excitation pulses is increased. If the homogeneous line shape is Lorentzian, the polarization decays as $\exp[-2\tau/T_2]$ and the signal intensity decays as $\exp[-4\tau/T_2]$ where T_2 is the homogeneous or transverse dephasing time. In addition to the dephasing induced by dynamics, population decay also contributes to the coherence loss. The pure dephasing time, T_2^* can be obtained by removing the population decay contribution.

In a stimulated echo, a pulse excites the chromophores as before but at time τ, the second pulse is split into two pulses separated by the interval T_w. The echo appears as a fourth pulse. The stimulated photon echo is sensitive to homogeneous dephasing during the interval τ between the first and second pulses and between the third and echo pulses. It is also sensitive to frequency fluctuations (spectral diffusion) that occur on the slower time scale, T_w.

Hole burning is a frequency domain line narrowing experiment. In a hole burning experiment, a narrow band laser excites a narrow transition frequency subset of the chromophores in the inhomogeneous line. A spectrum bracketing the point of excitation will show reduced absorption, the hole. Molecules that were excited by the laser can contribute to the hole, these being ones either initially on resonance with the laser, or ones that had fluctuations in energy during the hole burning period that brought them into resonance with the laser. In the time interval between burning and reading the hole, fluctuations in transition energies can bring molecules into the frequency region of the hole. Therefore, fluctuations in frequency that occur on the time scale from burning through reading the hole will determine the hole width. Since this time scale is typically long (seconds), the experiment will be sensitive to very slow dynamical processes (very slow spectral diffusion). It has been formally proven that hole burning is the frequency domain equivalent of the stimulated echo experiment [51,52]. The spectrum of the hole is determined by the Fourier transform of the stimulated echo correlation function. Hole burning is a frequency domain stimulated echo experiment. In a hole burning experiment, T_w is essentially the time required to do the experiment, from burning through reading. The typical time scale for a photon echo experiment is 100 ps. Fluctuations occurring on a μsec or msec time scale are static on the time scale of a photon echo experiment, and do not contribute to the measured dephasing time. In contrast, μsec and msec time scale fluctuations are rapid on the seconds time scale of a hole burning experiment, and contribute to the measured dephasing time. Therefore, echo and hole burning experiments should not measure the same dephasing

times in systems which have broad distributions of fluctuation rates. Changing T_w, the time scale of experiments, provides a path for the examination of dynamics over a very wide range of times from psec to 10,000 sec, or longer.

The dephasing time measured by photon echoes is substantially longer than the dephasing time measured by hole burning experiments [48]. The additional broadening of a hole arises from slow time scale spectral diffusion. At low temperature, the ratio of the hole line width to echo determined line width is proportional to the integral of the fluctuation rate distribution, P(R), from time scale of the homogeneous dephasing time to the time, T_w, associated with the hole burning experiment [52]. P(R) is the probability of having a dynamical process of rate R in the glass. Thus if T_w (time between burning and reading the hole) is varied over a range of times in which some rates are active, i. e., 1/R falls within the experimental time range, the holewidth will change. The change in holewidth can be used to quantitatively determine P(R).

Recently we performed experiments of this nature. We examined cresyl violet in ethanol, ethanol-d, and glycerol glasses and resorufin in ethanol [48-50]. For example, holes were measured at different times after burning in the cresyl violet/ethanol system. As the time between burning and reading increased, the hole broadens. For cresyl violet in ethanol at 1.30 K the holes broadened from 2.2 GHz to 3.2 GHz between 100 msec and 7000 sec. The holewidth was observed to vary over the entire range of study, but the change in width is most pronounced in the range of 50 seconds.

By performing a detailed theoretical analysis of the four time

correlation function for hole burning, the dependence of the hole width on the waiting time, T_w, was obtained. It is possible to determine the fluctuation rate distribution by examining the holewidth, or the dephasing time in time domain experiments, as a function of T_w. A log normal distribution (Gaussian on a log time scale) was found to be the form of P(R) that fit the data. At low temperatures, TLS relaxation is caused by phonon assisted tunneling. For this case, a log normal distribution of fluctuation rates is equivalent to a Gaussian distribution of tunneling parameters.

The experiments were repeated on resorufin in ethanol, and identical results were obtained. This proves that the dynamics in this time range are an intrinsic property of the glass, independent of the chromophore. Experiments on glycerol glass covering the same range of T_w displayed no hole broadening. Again demonstrating that the dynamics observed in ethanol glass is an intrinsic property of the glass and not a function of the experimental procedures.

The experiments described above used a conventional hole burning procedure, i. e., the hole was burned and following a time T_w, the hole was read out by sweeping the laser frequency. We have extended the measurements to T_ws (time between burning and reading) as fast as 10 μsec [49]. To accomplish this we measure the entire time response at a given frequency and then repeat this for a number of frequencies. This avoids the necessity of sweeping the reading frequency across the hole. To do this we employ a 300 MHz acousto-optic modulator (AOM). The narrow band dye laser beam is split, one part becomes the burning beam. This is passed through two AOMs which are used to turn it on and off rapidly to make the burning pulse. The other part of the dye laser beam

passes through the 300 MHz AOM. The diffracted beam is shifted from the burning beam by exactly 300 MHz. To read at 600 MHz, the diffracted beam is passed back through the AOM. The beam is again diffracted, and is now shifted 600 MHz from the burn frequency. This process can be repeated up to six time with a single AOM with more than sufficient intensity to read the hole. Thus reading frequencies of 0, 300, 600, 900, 1200, 1500, and 1800 MHz shift from the center frequency are obtained. This can be done on either side of the line by taking either the +1 or -1 diffraction order.

At each probe frequency the full time dependence is measured. The holes used are transient, presumably triplet bottle neck holes, which refill on the 100 msec time scale for creysl violet in ethanol. Therefore, about 1000 shots can be averaged to obtain good quality data. Great care is taken to test for saturation, heating and other unwanted side effects.

The holes at 10 μsec are 1.2 GHz compared to 3.2 GHz measured at 7000sec. Between 10 μsec and 100 msec the increase in width plotted on a log time scale is well fit by a straight line, indicating a $P(R) = 1/R$ distribution. Therefore, using hole burning we have examined hole widths from 10 μsec to 10,000 sec, i. e., over 9 decades of time.

On fast time scales we have employed photon echo and stimulated echo experiments [48,50]. The photon echo experiments demonstrates that the fluctuation rate distribution from 1 psec to 1 nsec also has the form $P(R) = 1/R$. Extrapolation of the msec to μsec hole burning data to the nsec time scale produces essentially perfect agreement with the photon echo data. This indicates that a 1/R distribution exists in ethanol from psecs to 100 msec, i. e., over 11 decades of time.

As discussed above, the hole burning experiments are the Fourier transform of the stimulated echo experiment. To work on fast time scales it is preferable to work in the time domain rather than the frequency domain. To extend the short time echo experiments to longer times, to avoid the necessity of doing very fast hole burning experiments, and to fill in the gap between μsec time scale hole burning experiments and psec time scale photon echo experiments, we are using the stimulated photon echo. Because of spectral diffusion on a fast time scale, the stimulated echo decay is faster than the two pulse echo decay. This is equivalent to the classic NMR experiments that compare spin echoes and stimulated echoes to measure spectral diffusion. The results confirm that P(R) is, in fact, 1/R for fast fluctuation rates.

The net result is the observation of hole broadening over 9 decades of time and the determination of the low temperature ethanol glass fluctuation rate distribution over 16 decades of time. The increase in observed dynamical line widths by a factor of approximately 8 from the psec time scale to the 10,000 sec time scale is caused by spectral diffusion induced by the fluctuating Two Level System structure of glasses. The data is analyzed using a detailed theoretical description of the four time correlation functions that describe the various line narrowing experiments.

E. Theory of Shock Induced Multiphonon Up-pumping

We have developed [53] a theory for vibrational up-pumping, defect hot spot formation, and the onset of chemistry induced by a shock wave in a solid composed of large organic molecules, e. g., RDX. The model and calculations describe the flow of energy in a shocked solid. The shock excites the bulk phonons, which rapidly achieve a state of phonon equilibrium characterized by a phonon quasi-temperature. The excess energy subsequently flows into the molecular vibrations, which are characterized by a vibrational quasi-temperature. The multiphonon up pumping process occurs because of anharmonic coupling terms in the solid state potential surface. Of central importance are the lowest energy molecular vibration, or "doorway" modes, through which mechanical energy enters and leaves the molecules. Using reasonable experimental parameters, it is found that the quasi-temperature increase of the internal molecular vibrations and equilibration between the phonons and vibrations is achieved on the time scale of a few tens of picoseconds. A new mechanism is presented for the generation of "hot spots" at defects. Defects are postulated to increase the anharmonic coupling in a localized area of the solid, causing the vibrational temperature in this area to briefly overshoot the bulk. The influence of the higher defect vibrational temperature on chemical reactivity is estimated. It is shown that even small increases in defect anharmonic coupling have profound effects on the probability of shock induced chemistry. The anharmonic defect model predicts a size effect. The defect enhanced chemical reaction probability is reduced as the particle size is reduced.

F. References

[1] K.A. Nelson, R. Casalegno, R.J.D. Miller, and M.D. Fayer, J. Chem. Phys. 77(3), 1144 (1982).

[2] R. Collier, L.B. Burkhardt, and L.H. Lin, *Optical Holography*, Ch. 9, (Academic, New York, 1971).

[3] H. Kogelnik, Bell Syst. Tech. J. 48, 2909 (1969).

[4] J.S. Meth, C.D. Marshall, and M.D. Fayer, Sol. State Comm., 74(4), 281 (1990).

[5] I.M. Fishman, C.D. Marshall, M.D. Fayer, J. Opt. Soc. Amer. B, and references therein, in press, publication scheduled for Sept. 1991.

[6] J. S. Meth, C. D. Marshall, and M. D. Fayer, J.Appl. Phys, 67(7), 3362 (1990).

[7] M. Marinelli, F. Murtas, M.G. Mecozzi, U. Zammit, R. Pizzoferrato, F. Scudieri, S. Martellucci, and M. Marinelli, Appl. Phys. A, 51, 387 (1990).

[8] S.E. Gustafson, Rev. Sci. Instrum., 62(2), 797 (1991).

[9] A. C. Eckbreth, *Laser Diagnostics for Combustion Temperature & Species*, (Abacus Press, Cambridge, MA, 1988).

[10] See for instance A. C. Eckbreth G. M. Dobbs, J. H. Stufflebeam, and P. A. Tellex, Appl. Opt. 23, 1328 (1984); B. Attal-Tretout and P. Bouchardy, La Rech. Aerosp. 5, 19 (1987).

[11] P. Ewart and S. V. O'Leary, Opt. Lett. 11, 279 (1986); P. Ewart, P. Snowdon, and I. Magnusson, Opt. Lett. 14, 563 (1989); T. Dreier and D. J. Rakestraw, Opt. Lett. 15, 72 (1990); T. Dreier and D. J. Rakestraw, Appl. Phys. B 50, 479 (1990); D. J. Rakestraw, R. L. Farrow, and T. Dreier, Opt. Lett. 15, 709 (1990).

[12] R. Trebino and L. R. Rahn, Opt. Lett. 12, 912 (1987)

[13] For general information on transient gratings, see H. J. Eichler, P. Günter, and D. W. Pohl, *Laser-Induced Dynamic Gratings* (Springer-Verlag, Berlin, 1986).

[14] T. S. Rose, W. L. Wilson, G. Wäckerle, and M. D. Fayer, J. Chem. Phys. **86**, 5370 (1987).

[15] J. T. Fourkas, T. R. Brewer, H. Kim, and M. D. Fayer, Opt. Lett. **16**, 177 (1991); J. T. Fourkas, T. R. Brewer, H. Kim, and M. D. Fayer, J. Chem. Phys., in press.

[16] B. P. Kibble, G. Koppley, and L. Krause, Phys. Rev. **153**, 9 (1967).

[17] H. J. Eichler, P. Günter, and D. W. Pohl, *Laser-Induced Dynamic Gratings*, (Springer-Verlag, Berlin, 1986).

[18] A. von Jena and H. E. Lessing, Opt. and Quant. Electron. **11**, 419 (1979).

[19] D. Kühlke, Appl. Phys. B **34**, 129 (1984).

[20] G. Eyring and M. D. Fayer, J. Chem. Phys. **81**, 4314 (1984).

[21] L. J. Rothberg and N. Bloembergen, Phys. Rev. A **30**, 820 (1984).

[22] T. K. Yee and T. K. Gustafson, Phys. Rev. A **18**, 1597 (1978).

[23] Y. Prior, IEEE J. Quant. Electron. **QE-20**, 37 (1984).

[24] M. D. Fayer, IEEE J. Quant. Electron. **QE-22**, 1437 (1986).

[25] J. T. Fourkas, R. Trebino, and M. D. Fayer, J. Chem. Phys., submitted.

[26] J. T. Fourkas, T. R. Brewer, H. Kim, and M. D. Fayer, Opt. Lett. **16**, 177 (1991); J. T. Fourkas, T. R. Brewer, H. Kim, and M. D. Fayer, J. Chem. Phys., in press.

[27] A. Abragam, *The Principles of Nuclear Magnetism* (Oxford U. Press, London, 1961).

[28] M. Mehring, *Principles of High-Resolution NMR in Solids*,

(Springer-Verlag, Berlin, 1983).

[29] A. H. Zewail, T. E. Orlowski, K. E. Jones, and D. E. Godar, *Chem Phys Lett.* **48**, 256-261 (1977).

[30] W. S. Warren and A. H. Zewail, *J. Chem. Phys.* **78**, 2279-2297 (1983).

[31] J. T. Fourkas, W. L. Wilson, G. Wäckerle, A. E. Frost, and M. D. Fayer, J. Opt. Soc. Am. B **6**, 1905-1910 (1989).

[32] S. Ruhman and K.A. Nelson, J. Chem. Phys. 94 (1991) 859.

[33] D. McMorrow, W.T. Lotshaw, and G.A. Kenney-Wallace, IEEE J. Quantum Electron. QE-24 (1988) 443.

[34] D. Kivelson, in *Rotational Dynamics of Small and Macromolecules*, edited by Th. Dorfmueller and R. Pecora (Springer, Berlin, 1987) p. 1.

[35] D. McMorrow, and W.T. Lotshaw, Chem. Phys. Lett. 174 (1990) 85.

[36] V.J. Newell, F.W. Deeg, S.R. Greenfield, and M.D. Fayer, J. Opt. Soc. Am. B 6 (1989) 257.

[37] G. Erying and M.D. Fayer, J. Chem. Phys. 81 (1984) 4314.

[38] J. Etchepare, G. Grillon, J.P. Chambaret, G. Harmoniaux, and A. Orszag, Opt. Comm. 63 (1987) 329.

[39] F.W. Deeg, and M.D. Fayer, J. Chem. Phys. 91 (1989) 2269.

[40] F.W. Deeg, J.J. Stankus, S.R. Greenfield, V.J. Newell, and M.D. Fayer, J. Chem. Phys. 90 (1989) 6893.

[41] F.W. Deeg, and M.D. Fayer, Chem. Phys. Lett. 167 (1990) 527.

[42] F.W. Deeg, and M.D. Fayer, J. Mol. Liq. 45 (1990) 19.

[43] F.W. Deeg, S.R. Greenfield, J.J. Stankus, V.J. Newell, and M.D. Fayer, J. Chem. Phys. 93 (1990) 3503.

[44] H.J. Coles, Mol. Cryst. Liq. Cryst. (Lett) 49 (1978) 67.

[45] S.R. Greenfield, OV, J.J. Stankus, and M.D. Fayer, in preparation.

G. Publications Supported by This Grant (N00014-89-J-1119)

1. "Solute-Solvent Dynamics and Interactions in Glassy Media: Photon Echo and Optical Hole Burning Studies of Cresyl Violet in Ethanol Glass," L. R. Narasimhan, Dee William Pack, and M. D. Fayer, Chem. Phys. Lett., 152, 287 (1988).

2. "Tunable Subpicosecond Dye Laser Amplified at 1 KHz by a Cavity-Dumped, Q-Switched and Mode-Locked Nd:YAG Laser," V. J. Newell, F. W. Deeg, S. R. Greenfield, and M. D. Fayer, J. Optical Soc. Am. B, 6, 257 (1989).

3. "A New Approach to the Nonlinear Spectroscopic Investigation of Dynamics in Complex Solids: Theory and Experiments," Y. S. Bai and M. D. Fayer, Comments on Condensed Matter Physics, 14, pp. 343-364. Gordon and Breach, Science Publishers, Inc., Great Britain (1989).

4. "Analysis of Complex Molecular Dynamics in an Organic Liquid by Polarization Selective Subpicosecond Transient Grating Experiments,"F. W. Deeg and M. D. Fayer, J. Chem. Phys., 91, 2269 (1989).

5. "Anisotropic Reorientational Relaxation of Biphenyl: Transient Grating Optical Kerr Effect Measurements," F. W. Deeg, John J.Stankus, S. R. Greenfield, Vincent J. Newell, and M. D. Fayer, J. Chem. Phys., 90, 6893, (1989).

6. "Picosecond Time Scale Phase-Related Optical Pulses: Measurement of Na Optical Coherence Decay by Observation of Incoherent Fluorescence," John T. Fourkas, William L. Wilson, G. WE. Frost, and M. D. Fayer, J. Optical Soc. Am. B, 6, 1905 (1989).

7. "Probing Organic Glasses at Low Temperature with Variable Time Scale Optical Dephasing Measurements," L. R. Narasimhan, K. A. Littau, Dee William Pack, Y. S. Bai, A. Elschner, and M. D. Fayer, Chemical Rev. 90, 439 (1990).

8. "Shocked Molecular Solids: Vibrational Up Pumping, Defect Hot Spot Formation, and the Onset of Chemistry," Dana D. Dlott and M. D. Fayer, J. Chem. Phys., 92, 3798 (1990).

9. "Low Temperature Glass Dynamics Probed by Optical Dephasing Measurements," L. R. Narasimhan, K. A. Littau, Y. S. Bai, Dee William Pack, A. Elschner, and M. D. Fayer, J. Luminescence, 45, 49 (1990).

10. "The Nature of Glass Dynamics: Thermal Reversibility of Spectral Diffusion in a Low Temperature Glass," Y. S. Bai, K. A. Littau, and M. D. Fayer, Chem. Phys. Lett., 162, 449 (1989).

11. "Dynamics in the Pretransitional Isotropic Phase of Pentylcyanobiphenyl Studied with Subpicosecond Transient Grating Experiments," F. W. Deeg and M. D. Fayer, Chem. Phys. Lett., 167, 527 (1990).

12. "Two-Level Systems and Low-Temperature Glass Dynamics: Spectral Diffusion and Thermal Reversibility of Hole-Burning Linewidths," K. A. Littau, Y. S. Bai, and M. D. Fayer, J. Chem. Phys., 92, 4145 (1990).

13. "Nonhydrodynamic Molecular Motions in a Complex Liquid: Temperature Dependent Dynamics in Pentylcyanobiphenyl," F. W. Deeg, S. R. Greenfield, John J. Stankus, Vincent J. Newell, and M. D. Fayer, J. Chem. Phys., 93, 3503 (1990).

14. "Picosecond Photon Echo Experiments Using a Superconducting Accelerator Pumped Free Electron Laser," Y. S. Bai, S. R. Greenfield, M. D. Fayer, T. I. Smith, J. C. Frisch, R. L. Swent, and H. A. Schwettman, J. Opt. Soc. America B, J.O.S.A.B., 8, 1652 (1991).

15. "Optical Dephasing of a Near Infrared Dye in PMMA: Photon Echoes Using the Superconducting Accelerator Pumped Free Electron Laser," S. R. Greenfield, Y. S. Bai, and M. D. Fayer, Chem. Phys. Lett., 170, 133 (1990).

16. "Transient Grating Optical Kerr Effect Measurements of Reorientational Dynamics in Liquids and Liquid Crystaline Samples," F. W. Deeg and M. D. Fayer, J. Mol. Liquids, 45, 19 (1990).

17. "Probing Low Temperature Glass Dynamics by Fast Generation and Detection of Optical Holes," K. A. Littau and M. D. Fayer, Chem. Phys. Lett., 176, 551 (1991).

18. "Picosecond Time-Resolved Four Wave Mixing Experiments in Sodium-Seeded Flames," John T. Fourkas, Timothy R. Brewer, Hackjin Kim, and M. D. Fayer, Optics Letters, 16, 177 (1991).

19. "Surface Selectivity in Four Wave Mixing: Transient Gratings as a Theoretical and Experimental Example," I. M. Fishman, C. D. Marshall, J. S. Meth, and M. D. Fayer, J.O.S.A.B, 8, 1880 (1991).

20. "Picosecond Polarization-selective Transient Grating Experiments in Sodium-seeded Flames," John T. Fourkas, Timothy R. Brewer, Hackjin Kim, and M. D. Fayer, J. Chem. Phys. 95, 5775 (1991).